Ezh2 variant orchestrates cholesterol biosynthesis via epigenetic regulation in mouse cerebellum

Fei Guan [1,2,3†], Zongyan Jiang[1,2,3†], Ye Tian[1,2,3], Bijun Jiang[1,2,3], Yixian Fan[1,2,3], Huamin Liang[1,2,3], Jing Jin[4*], Ying Yin[1,2,3,5*], Ximiao He[1,2,3,5*]

[1] Department of Physiology, School of Basic Medical Science, Huazhong University of Science and Technology, Wuhan 430030, Hubei, China.
[2] Center for Genomics and Proteomics Research, School of Basic Medicine, Tongji Medical College, Huazhong University of Science and Technology, Wuhan 430030, Hubei, China
[3] Hubei Key Laboratory of Drug Target Research and Pharmacodynamic Evaluation, Huazhong University of Science and Technology, Wuhan 430030, Hubei, China.
[4] National Demonstration Center for Experimental Basic Medical Education, School of Basic Medicine, Tongji Medical College, Huazhong University of Science and Technology, Wuhan 430030, China;
[5] Key Laboratory of Vascular Aging, Ministry of Education, Tongji Hospital, Tongji Medical College, Huazhong University of Science and Technology, Wuhan 430030, Hubei, China

[†]These authors have contributed equally to this work.
*** Correspondence:**
Corresponding Authors
Ximiao He: XimiaoHe@hust.edu.cn
Ying Yin: YinYing@hust.edu.cn
Jing Jin: JinJng@hust.edu.cn

Running title: *Ezh2* variant in cerebellar cholesterol metabolism

Keywords: cerebellum, *Ezh2*, alternative splicing, multi-omics, epigenetics, cholesterol, astroglia

Materials and Methods

Animals

The mice used in this study were of mixed genetic backgrounds (C57BL/6J and FVB). All mice were group-housed (3-5 mice per cage) in SPF grade experimental animal centers housing on a 12-hour light/12-hour dark cycle and allowed to eat and drink ad libitum. Mutant mice were generated as previously described[1]. These heterozygous mutant mice were further inbred to obtain homozygous mutant mice, and their wild-type littermates were used as control. All the experimental procedures with mice were performed in accordance with the animal guidelines approved by the Institutional Animal Care and Use Committee of Huazhong University of Science and Technology. Genotyping for *Ezh2*$^{Long-/-}$ mice was performed using the two primer pairs listed in Supplementary Table S1.

To restore cholesterol biogenesis, mice received intraperitoneal injections of valproic acid sodium salt (Sigma-Aldrich, 676380) at a dose of 30 mg/kg, while the control group received an equal volume of saline. The injections were administered ten times at 48 h intervals, as previously described[2].

Behavioral Testing

All behavioral experiments were conducted using male mice beginning at 9 weeks of age, with most testing completed by 12 weeks. Prior to behavioral assessments, animals were habituated through twice-daily 15 min handling sessions for 3 consecutive days. Before each test session, mice were transported to the testing room and allowed 30 minutes for environmental acclimation. Standardized cleaning procedures were implemented between trials, with all apparatus surfaces thoroughly wiped with 70% ethanol to eliminate residual odor cues, unless otherwise specified. Throughout behavioral testing, experimenters remained blinded to the genotype of all mice.

Open field test

Spontaneous locomotor activity was evaluated in a white opaque square arena (45 × 45 × 45 cm), where individual mice were placed in the center and allowed to freely explore for 10 min. Movement parameters including total distance traveled, movement trajectory, and time spent in the center versus peripheral zones were captured and analyzed by the Supermaze 2.0 video tracking system (Softmaze, China). Data from the first minute were excluded from analysis.

Elevated plus maze test

The elevated plus maze, consisting of two open arms and two enclosed arms extending from a central platform, was positioned 40 cm above ground level to assess anxiety-like behavior. Each mouse was placed in the center zone facing an open arm and allowed to freely explore the apparatus for 10 min. Behavioral parameters including time spent in open versus closed arms, arm entries, and total distance traveled were automatically recorded using the Supermaze 2.0 video tracking system (Softmaze, China). The first minute of data was excluded prior to analysis.

Novel object recognition test

The procedure was performed as previously described with modification[3]. The day before the experiment began, mice were habituated for 10 min in an empty white opaque square chamber (45 × 45 × 45 cm). The following day, two identical clear cylinders were placed in the opposite corners

of the testing chamber for training session. Each mouse was introduced to the arena facing away from the objects and allowed to explore freely for 10 min. After a 1 h retention interval, one object was replaced with a novel yellow square for the 10 min testing trial. Exploration behavior was recorded and defined as either direct nose contact with an object or front paws positioned within 3 cm of an object. The percentage of discrimination index (DI) was calculated as follows: DI=Tn / (Tf + Tn) × 100%; Tn: novel object exploration time; Tf: familiar object exploration time.

Morris water maze test

Spatial learning and memory were evaluated for rodents in the Morris water maze[4]. The MWM system setup consisted of a 120 cm diameter circular pool surround by visual cues and filled with water (23 ± 2 °C) made opaque by nontoxic paint. Mice were trained to locate a 10 cm diameter hidden platform, submerged 1 cm below the water surface in the center of one of the pool quadrants, based on distal visual cues to escape from the pool. Mice received training trials from starting points of 4 different quadrants for 1 min each day, with 1 h interval between training rounds, for 6 consecutive days. The escape latency of 4 training sessions per day were averaged. The next day, the platform was removed, and a spatial probe trial was conducted to assess memory retention. For each probe trial, mice were introduced into the pool from the quadrant diagonally opposite to the original platform location. The TMV-100S video tracking system (TaiMeng, China) automatically quantified spatial memory parameters including target quadrant occupancy time, platform zone crossings, and swim path trajectories during the 1 min test period.

Animal Procedures and Tissue Preparation

The mice were deeply anesthetized with tribromoethanol (AibeiBio, M2910) by intraperitoneal injection. For tissue collection intended for molecular analysis, animals were transcardially perfused with ice-cold phosphate-buffered saline (PBS). The brains were rapidly extracted, and the cerebellum was dissected, snap-frozen in liquid nitrogen, and stored at -80°C for further processing.

Isolation of primary cerebellar astrocytes

Acute isolation of primary astrocytes from WT and *Ezh2*$^{\text{Long-/-}}$ mice was performed using a combination of enzymatic and mechanical dissociation as described previously[5]. In brief, freshly dissected cerebellar tissues were minced and digested using the Adult Brain Dissociation Kit (Miltenyi Biotec, 130-107-677) according to the manufacturer's instructions. Tissue dissociation was processed using the gentleMACS Octo Dissociator (Miltenyi Biotec, 130-096-427) with predefined program '37C_ABDK_02'. The resulting suspension was sequentially filtered through a 70-μm MACS SmartStrainer (Miltenyi Biotec, 130-098-462) to remove undissociated tissues, followed by debris and erythrocytes removal. Purified cell suspension was then incubated with Anti-ACSA-2 MicroBeads (Miltenyi Biotec, 130-097-679) for magnetic labeling of astrocytes. Labeled cells were positively selected using an MS Column (Miltenyi Biotec, 130-042-201) placed within a MACS Separator. The ACSA-2^{+} cells were eluted as the purified astrocyte fraction and immediately processed for downstream applications.

Flow cytometry

Primary astrocytes were analyzed for purity by ID7000 Spectral Cell Analyzer (Sony Biotechnology,

Japan) using PE-conjugated anti-ACSA-2 (Miltenyi Biotec, 130-123-284) at manufacturer's recommended concentration. Data analysis was performed with FlowJo (version 10.9.0).

RNA isolation and reverse transcription-quantitative PCR

Total RNA was extracted from primary astrocytes or tissue samples using the FastPure Cell/Tissue Total RNA Isolation Kit (Vazyme, RC112-01), following the manufacturer's instructions. RNA concentration and purity were determined using a NanoDrop2000 (Thermo Fisher Scientific, USA) spectrophotometer. cDNA was synthesized from equal amounts of total RNA using the HiScript III All-in-one RT SuperMix (Vazyme, R333-01). Genomic DNA contamination was monitored by including no-RT control reactions. Quantitative real-time PCR was performed using Taq Pro Universal SYBR qPCR Master Mix (Vazyme, Q712-02) on a Quantagene q225 Real-Time PCR machine (Kubo Technology, China). Gene expression levels were normalized to *Gapdh* and calculated using the comparative CT (ΔΔCT) method. The primer sequences used are listed in Supplementary Table S1.

Protein extraction and Western blot analysis

Tissue samples were harvested and lysed in RIPA buffer (Beyotime, P0013B) supplemented with Protease and Phosphatase inhibitor cocktail. After incubated on ice for 30 min, lysates were subjected to sonication using 6 cycles of 5 s on/5 s off to ensure complete disruption. The samples were centrifuged at 14,000 × g for 15 min at 4°C, and the resulting supernatants were collected as total protein. Protein concentrations were determined by BCA Kit (Beyotime, P0012S). Equal amounts of protein samples were separated by SDS-PAGE and then transferred to PVDF membranes. Subsequently, the membranes were blocked with 5% non-fat milk in 1XTBST for 1 h at room temperature, followed by incubation with primary antibody overnight at 4°C. Finally, membranes were incubated with host-specific near-infrared fluorescently labeled secondary antibody for 1 h at room temperature in the dark. Signals were visualized by the LI-COR Odyssey imaging system (LI-COR Biosciences, USA).

The following antibodies were used: rabbit anti-EZH2 (Active Motif, 61641), rabbit anti-HMGCS1 (Proteintech, 17643-1-AP), rabbit anti-CYP51 (Proteintech, 13431-1-AP), mouse anti-GGPS1 (Santa Cruz, sc-271680), rabbit anti-SREBP2 (Cayman, 10007663), rabbit anti-H3K27me3 (Active Motif, 39055), rabbit anti-H3K27ac (Abcam, ab4729), rabbit anti-MAG (Boster, A03019), rabbit anti-MBP (Proteintech, 10458-1-AP), rabbit anti-PLP (Huabio, HA500202), mouse anti-H3 (Proteintech, 68345-1-Ig), rabbit anti-GAPDH (ABclonal, A19056), goat anti-rabbit IgG (Immunoway, RS23920), goat anti-mouse IgG (Immunoway, RS23710).

Cholesterol quantification assay

Total or free cholesterol levels were measured in brain tissues, primary astrocytes, and plasma samples from WT and *Ezh2*$^{Long-/-}$ mice. For tissue analysis, samples (10 mg) were homogenized in 200 μL of lipid extraction buffer (chloroform: isopropanol: NP-40, 7:11:0.1) and centrifuged at 15,000 × g for 10 min. The supernatant was air-dried at 50ºC to evaporate organic solvents. For cellular cholesterol measurement, pelleted cells (10^6 cells) were similarly processed using 200 μL of extraction buffer. Blood samples were collected via retro-orbital bleeding into EDTA-coated tubes to prevent coagulation. After centrifugation at 2,000 × g for 10 min at 4°C, the plasma supernatant was collected. Cholesterol concentrations were determined spectrophotometrically

using Total Cholesterol Assay Kits (Cell Biolabs, STA-384), with all the samples diluted 1:50 prior to measurement. All procedures were performed according to the manufacturer's protocols.

Sterol extraction and analysis

Mouse cerebellar sterols were quantified by a targeted sterolomics approach based on Ultra-Performance Liquid Chromatography-Tandem Mass Spectrometry (UPLC-MS/MS). Lipid extraction from cerebellum was performed using a modified Bligh and Dyer extraction procedure as previously described[6]. The lipid extracts were resuspended in 500 µL ethanol containing 5 µg butylated hydroxytoluene (BHT) as an antioxidant, along with a 50 µL internal standard cocktail consisting of d_6-lanosterol, d_5-zymosterol, d_7-lathosterol, d_7-7-dehydrocholesterol, d_7-sitosterol, and d_6-cholesterol (Avanti Polar Lipids). Samples were incubated at 4°C with 1,200 rpm for 15 min. After incubation, 250 µL Milli-Q water and 1 mL n-hexane were added, followed by vortexing and centrifugation at 12,000 rpm for 5 min at 4°C. The upper n-hexane phase, containing oxysterols and cholesterol, was transferred to a fresh tube. The extraction was repeated with an additional 1 mL n-hexane, and the combined organic phases were dried under vacuum (SpeedVac, organic mode). Cholesterol and derivatives were subjected to picolinoyl derivatization to improve ionization prior to UPLC-MS/MS analysis using a Shimadzu 40X3B-UPLC/Sciex QTRAP 6500 Plus system. Quantification employed deuterated internal standards for precision.

Bulk RNA-seq library preparation and data analysis

Total RNA was extracted from WT and *Ezh2*$^{Long-/-}$ mice cerebellum and RNA integrity (RIN) was assessed using the Bioanalyzer 2100 system (Agilent Technologies, USA). Bulk sequencing libraries were prepared as follows. Isolated total RNA from each sample was subjected to poly(A) selection using poly-T oligo-attached magnetic beads. The enriched mRNA was fragmented and then used for synthesis of the first-strand cDNA using random hexamer primers and M-MuLV Reverse Transcriptase (RNase H-), followed by second-strand synthesis with DNA Polymerase I and RNase H for library construction. Qualified library preparations were then pooled, and sequencing was performed on an Illumina NovaSeq platform at the Novogene Bioinformatics Institute (Novogene, China).

Raw sequencing reads were filtered by Trim Galore (version 0.6.7) with default parameters to remove adapter contaminants and low-quality bases. The cleaned reads were then aligned to the mouse reference genome (mm10) using STAR aligner (version 2.7.5b)[7], and '--quantMode TranscriptomeSAM GeneCounts' for simultaneous alignment and quantification. Differential expression analysis was performed using DESeq2 package (version 1.42.1)[8] with significance thresholds set at absolute log2 fold change ≥ 0.5 and adjusted *p*-value (*P*adj) < 0.05.

snRNA-seq library preparation and data analysis

For each group (WT and *Ezh2*$^{Long-/-}$), cerebellar tissues from three genotype-matched mice were pooled per sequencing sample to ensure biological robustness and minimize individual variability. The mixed tissues were processed to isolate cell nuclei using an established protocol with minor modifications[9]. Briefly, frozen tissues were homogenized in Nuclei Lysis Buffer (NLB) containing 250 mM sucrose, 10 mM Tris-HCl, 3 mM MgAc2, 0.1% Triton X-100, 0.1 mM EDTA, and 0.2 U/µL RNase inhibitor. Nuclei were then purified through a discontinuous sucrose gradient centrifugation. Finally, the nuclei concentration was adjusted to ~1,000 nuclei/µL for snRNA-seq.

Single-nucleus libraries were constructed using the Chromium Single Cell 3' Reagent Kits (10x Genomics, version 3.1) according to the manufacturer's protocol. Library quantification was performed using the Qubit High Sensitivity DNA assay (Thermo Fisher Scientific, USA), followed by quality assessment with the Agilent 2200 Bioanalyzer system. Qualified libraries were then pooled in equimolar ratios for 150 bp paired-end sequencing on an Illumina NovaSeq 6000 platform. Raw sequencing reads were aligned to the mm10 mouse reference genome using Cell Ranger pipeline (version 6.1.2) with default parameters, including '--include-introns' and '--expect-cells = 5000' for nuclear RNA quantification and cell calling. The snRNA-seq feature-barcode matrices were processed by the Seurat package (version 5.1.0)[10]. Nuclei with fewer than 1,500 unique molecular identifiers (UMIs), over 8,000 or below 1,000 expressed genes, over 5% mitochondrial UMIs, and log10(UMIs of per gene) lower than 0.8 were removed. In subsequent analysis, erythrocyte-specific genes, mitochondrial genes, and genes that were detected in fewer than ten nuclei were excluded. Library-size normalization was performed by scaling transcript counts per cell to 10,000, followed by log2 transformation after adding a pseudocount of 1. The first 23 principal components were used for all cell clustering with a resolution at 1.5, yielding 35 preliminary clusters. These were further refined by merging several clusters based on shared marker gene expression patterns. For the clustering of lineage-specific subpopulations, astroglia were clustered using the top 12 principal components (resolution = 0.3), while oligodendrocytes utilized 9 principal components (resolution = 0.6). DEGs between WT and *Ezh2*$^{Long-/-}$ groups in the major cell populations were identified with the Wilcoxon Rank Sum test and Bonferroni correction using the Seurat's FindMarkers function. Significant DEGs were assessed from genes with a cutoff: minimum expression in 10% of cells in either population, absolute log2 fold change ≥ 0.25, and adjusted *p*-value (*P*adj) < 0.05.

ATAC-seq library preparation and data analysis

ATAC-seq libraries were prepared using the TruePrep DNA Library Prep Kit V2 for Illumina (Vazyme, TD501-01) following the manufacturer's protocol with minor optimizations. In short, nuclei were isolated from frozen tissue using NLB lysis followed by Dounce homogenization and sucrose gradient centrifugation. Isolated nuclei (50,000 per sample) were transposed using TruePrep Tagment Enzyme at 37°C for 30 min, followed by DNA purification using the FastPure Gel DNA Extraction Mini Kit (Vazyme, DC301-01). Tagmented DNA was amplified using TruePrep Amplify Enzyme for 11 cycles and amplified products were purified using VAHTS DNA Clean Beads (Vazyme, N411-01). Fragment distribution was assessed by Agilent 2100 Bioanalyzer and final libraries were sequenced on an Illumina NovaSeq platform.

ATAC-seq reads were quality and adaptor trimmed using Trim Galore (version 0.6.7) with default parameters. Cleaned reads were then aligned to the mm10 reference genome using Bowtie2 (version 2.5.0)[11] with the following parameters: --end-to-end --very-sensitive -X 2000 --no-unal --phred33. The resulting BAM files were filtered using Samtools (version 1.15.1)[12] with parameters '-q 20 -f 3 -F 268' to retain only uniquely mapped, properly paired reads. Additionally, mitochondrial reads were excluded to avoid potential artifacts from high mitochondrial DNA content. PCR duplicates were subsequently removed using Picard MarkDuplicates function (version 2.26.0). MACS2 (version 2.2.7.1) was used for peak calling with the parameter '-B --SPMR --nomodel --shift -100 --extsize 200 -q 0.05' for paired-end reads.

CUT&Tag-seq library preparation and data analysis

CUT&Tag assays were performed using Hyperactive Universal CUT&Tag Assay Kit for Illumina (Vazyme, TD903-01) according to the manufacturer's instructions with minor modifications. A total of 100,000 nuclei isolated from WT and *Ezh2*$^{Long-/-}$ mice cerebellum were cross-linked with 0.1% formaldehyde for 2 min at room temperature, followed by quenching with 2.5 M glycine for 5 min at room temperature. Nuclei were bound to concanavalin A-coated magnetic beads and incubated with target-specific primary antibody (1:50 dilution) overnight at 4°C. After washing, samples were treated with secondary antibody (1:100 dilution) for 1 h at room temperature, followed by incubation with 0.04 μM Hyperactive Protein A/G-Transposon for 1 h at room temperature. Tagmentation was initiated by adding Trueprep Tagment Buffer L and incubating at 37°C for 60 min. Libraries were constructed using the TruePrep Index Kit V2 for Illumina (Vazyme, TD202), with PCR cycles optimized for each target: 11 cycles for histone modifications (H3K27ac and H3K27me3) and 13 cycles for SREBP2 CUT&Tag. Final PCR products were purified with VAHTS DNA Clean Beads (Vazyme, N411-01). Paired-end sequencing was performed on an Illumina NovaSeq platform. Antibodies used include normal rabbit IgG (Cell Signaling, 2729), rabbit anti-SREBP2 (Cayman, 10007663), rabbit anti-H3K27me3 (Active Motif, 39055), rabbit anti-H3K27ac (Abcam, ab4729). Following adapter trimming with Trim Galore (version 0.6.7) using default parameters, quality-filtered reads were aligned to the mm10 genome using Bowtie2 (version 2.5.0) with setting parameters '--end-to-end --very-sensitive -I 10 -X 1000 --no-mixed --no-discordant --no-unal --phred33'. Post-alignment filtering was performed to retain uniquely mapped read pairs while systematically removing mitochondrial genome alignments. After duplicate removal, peaks were identified using MACS2 (version 2.2.7.1) with distinct parameters: narrowPeak (-B --SPMR -q 0.001) for H3K27ac and SREBP2, and broadPeak (-B --SPMR --broad --broad-cutoff 0.1) for H3K27me3. Genomic annotation was performed with ChIPpeakAnno (version 3.36.1), assigning peaks to the nearest gene and defining promoters as ± 1.5 kb surrounding TSS. Bigwig coverage files were generated using deepTools (version 3.5.4)[13], which were subsequently used for visualization and for obtaining average signal profiles. Differential binding analysis of SREBP2 was performed using DiffBind package (version 3.12.0) with default parameters.

Statistical analysis

All statistical analyses were conducted using R (version 4.3.2) or GraphPad Prism (version 9.0.0), with sample sizes and statistical methods detailed in the figure legends. Unless otherwise specified, between-group comparisons were assessed by two-tailed unpaired Student's t test. For multiple-group comparisons, one-way ANOVA with Dunnett's post hoc test or two-way ANOVA with Šídák's post hoc test were applied. Data were presented as mean ± SEM. Differences were considered to be statistically significant when p-value < 0.05.

Data Availability Statement

Source data for the figures are provided with the paper, and additional relevant data are available from the corresponding author upon reasonable request. Genomic datasets presented in this study, including RNA-seq, CUT&Tag-seq, ATAC-seq and snRNA-seq were uploaded to the National Genomics Data Center under the accession number CRA024737.

References

1. Guo, S.-M., Liu, X.-P., Tian, Q., Fei, C.-F., Zhang, Y.-R., Li, Z.-M., Yin, Y., He, X., and Zhou, L.-Q. (2022). Regulatory roles of alternative splicing at Ezh2 gene in mouse oocytes. Reproductive Biology and Endocrinology : RB&E *20*, 99. 10.1186/s12958-022-00962-x.
2. Zhu, X., Yao, Y., Hu, Y., Yang, J., Zhang, C., He, Y., Zhang, A., Liu, X., Zhang, C., and Gan, G. (2021). Valproic acid suppresses cuprizone-induced hippocampal demyelination and anxiety-like behavior by promoting cholesterol biosynthesis. Neurobiol Dis *158*, 105489. 10.1016/j.nbd.2021.105489.
3. Cai, Y., Tang, X., Chen, X., Li, X., Wang, Y., Bao, X., Wang, L., Sun, D., Zhao, J., Xing, Y., et al. (2018). Liver X receptor β regulates the development of the dentate gyrus and autistic-like behavior in the mouse. Proc Natl Acad Sci U S A *115*, E2725-E2733. 10.1073/pnas.1800184115.
4. Vorhees, C.V., and Williams, M.T. (2006). Morris water maze: procedures for assessing spatial and related forms of learning and memory. Nat Protoc *1*, 848-858.
5. Holt, L.M., Stoyanof, S.T., and Olsen, M.L. (2019). Magnetic Cell Sorting for In Vivo and In Vitro Astrocyte, Neuron, and Microglia Analysis. Curr Protoc Neurosci *88*, e71. 10.1002/cpns.71.
6. Song, J.-W., Lam, S.M., Fan, X., Cao, W.-J., Wang, S.-Y., Tian, H., Chua, G.H., Zhang, C., Meng, F.-P., Xu, Z., et al. (2020). Omics-Driven Systems Interrogation of Metabolic Dysregulation in COVID-19 Pathogenesis. Cell Metab *32*. 10.1016/j.cmet.2020.06.016.
7. Dobin, A., Davis, C.A., Schlesinger, F., Drenkow, J., Zaleski, C., Jha, S., Batut, P., Chaisson, M., and Gingeras, T.R. (2013). STAR: ultrafast universal RNA-seq aligner. Bioinformatics *29*, 15-21. 10.1093/bioinformatics/bts635.
8. Love, M.I., Huber, W., and Anders, S. (2014). Moderated estimation of fold change and dispersion for RNA-seq data with DESeq2. Genome Biol *15*, 550.
9. Krishnaswami, S.R., Grindberg, R.V., Novotny, M., Venepally, P., Lacar, B., Bhutani, K., Linker, S.B., Pham, S., Erwin, J.A., Miller, J.A., et al. (2016). Using single nuclei for RNA-seq to capture the transcriptome of postmortem neurons. Nat Protoc *11*, 499-524. 10.1038/nprot.2016.015.
10. Hao, Y., Stuart, T., Kowalski, M.H., Choudhary, S., Hoffman, P., Hartman, A., Srivastava, A., Molla, G., Madad, S., Fernandez-Granda, C., and Satija, R. (2024). Dictionary learning for integrative, multimodal and scalable single-cell analysis. Nat Biotechnol *42*, 293-304. 10.1038/s41587-023-01767-y.
11. Langmead, B., and Salzberg, S.L. (2012). Fast gapped-read alignment with Bowtie 2. Nat Methods *9*, 357-359. 10.1038/nmeth.1923.
12. Li, H., Handsaker, B., Wysoker, A., Fennell, T., Ruan, J., Homer, N., Marth, G., Abecasis, G., and Durbin, R. (2009). The Sequence Alignment/Map format and SAMtools. Bioinformatics *25*, 2078-2079. 10.1093/bioinformatics/btp352.
13. Ramírez, F., Ryan, D.P., Grüning, B., Bhardwaj, V., Kilpert, F., Richter, A.S., Heyne, S., Dündar, F., and Manke, T. (2016). deepTools2: a next generation web server for deep-sequencing data analysis. Nucleic Acids Res *44*, W160-W165. 10.1093/nar/gkw257.

Supplementary Figure and Legends

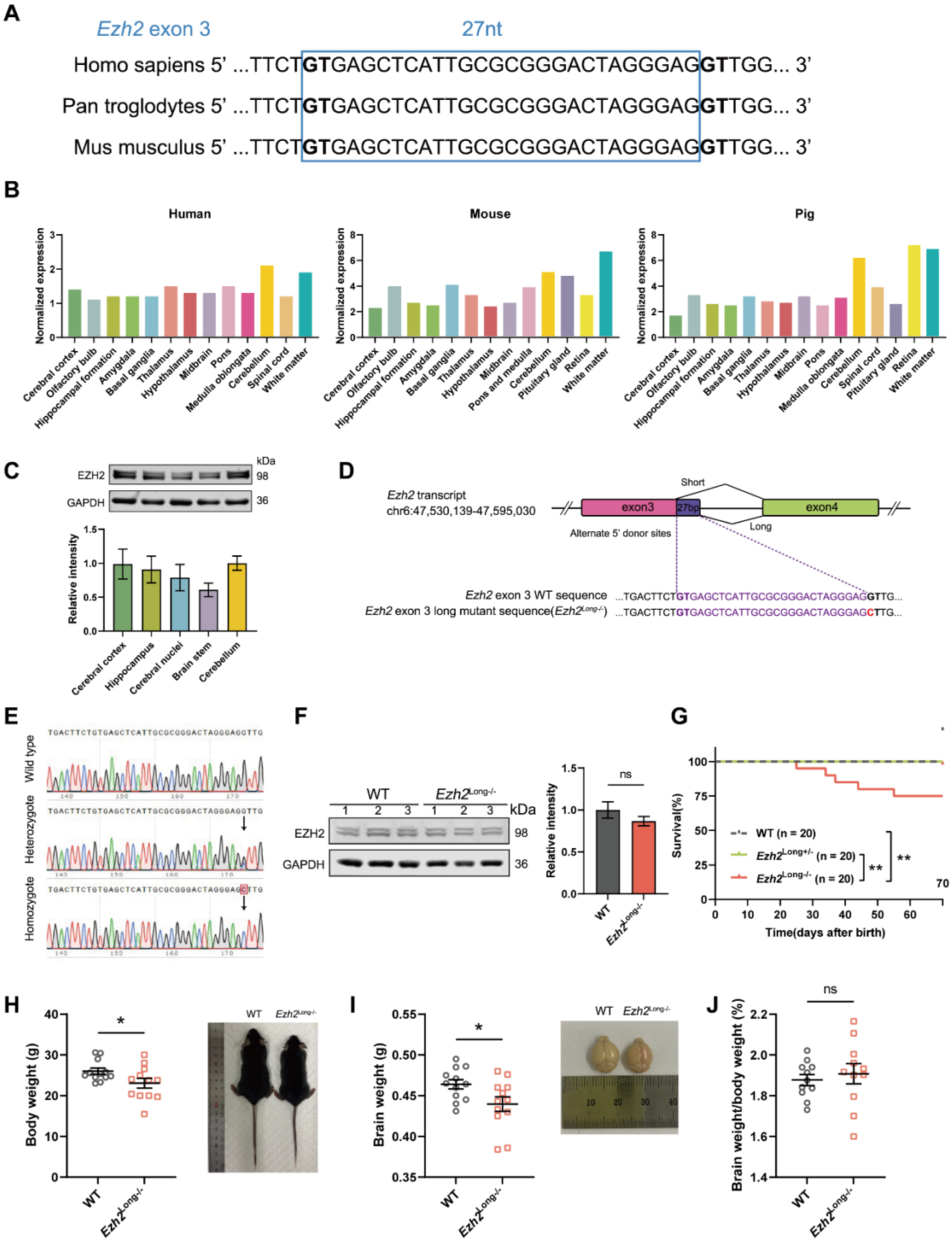

Figure S1. Generation strategy for *Ezh2*$^{Long-/-}$ mice.

(A) Conservation analysis of the alternative splicing site at the *Ezh2* gene loci across species revealed a 27-nt sequence (boxed) encoding nine additional amino acids in the long isoform, with the donor splice site 'GT' highlighted in bold. **(B)** Normalized mRNA expression profile of *Ezh2* in multiple brain regions of different species. Values were retrieved from the Human Protein Atlas (HPA, www.proteinatlas.org) using the consensus dataset. **(C)** Western blot analysis and quantification of EZH2 in different brain regions of WT (n = 4) mice. GAPDH was used as loading control. One-way ANOVA; ns, not significant. **(D)** Mutation strategy at *Ezh2* alternative splicing site: red-labelled mutated DNA sequences blocked alternate donor site to generate *Ezh2* exon 3 long

isoform deficiency mice. **(E)** Sanger sequencing validated base sequence of mouse point mutations. **(F)** Western blot analysis and quantification of EZH2 in isolated WT (n = 3) and *Ezh2*$^{Long-/-}$ (n = 3) cerebellums. GAPDH was used as loading control. Unpaired t test; ns, not significant. **(G)** Postnatal survival curve of WT and *Ezh2*$^{Long-/-}$ mice. Log-rank (Mantel-Cox) test; $^{**}p < 0.01$. **(H-J)** Representative images of the bodies (**H**) and brains (**I**) of the WT and *Ezh2*$^{Long-/-}$ mice at adult. Unpaired t test; $^{*}p < 0.05$.

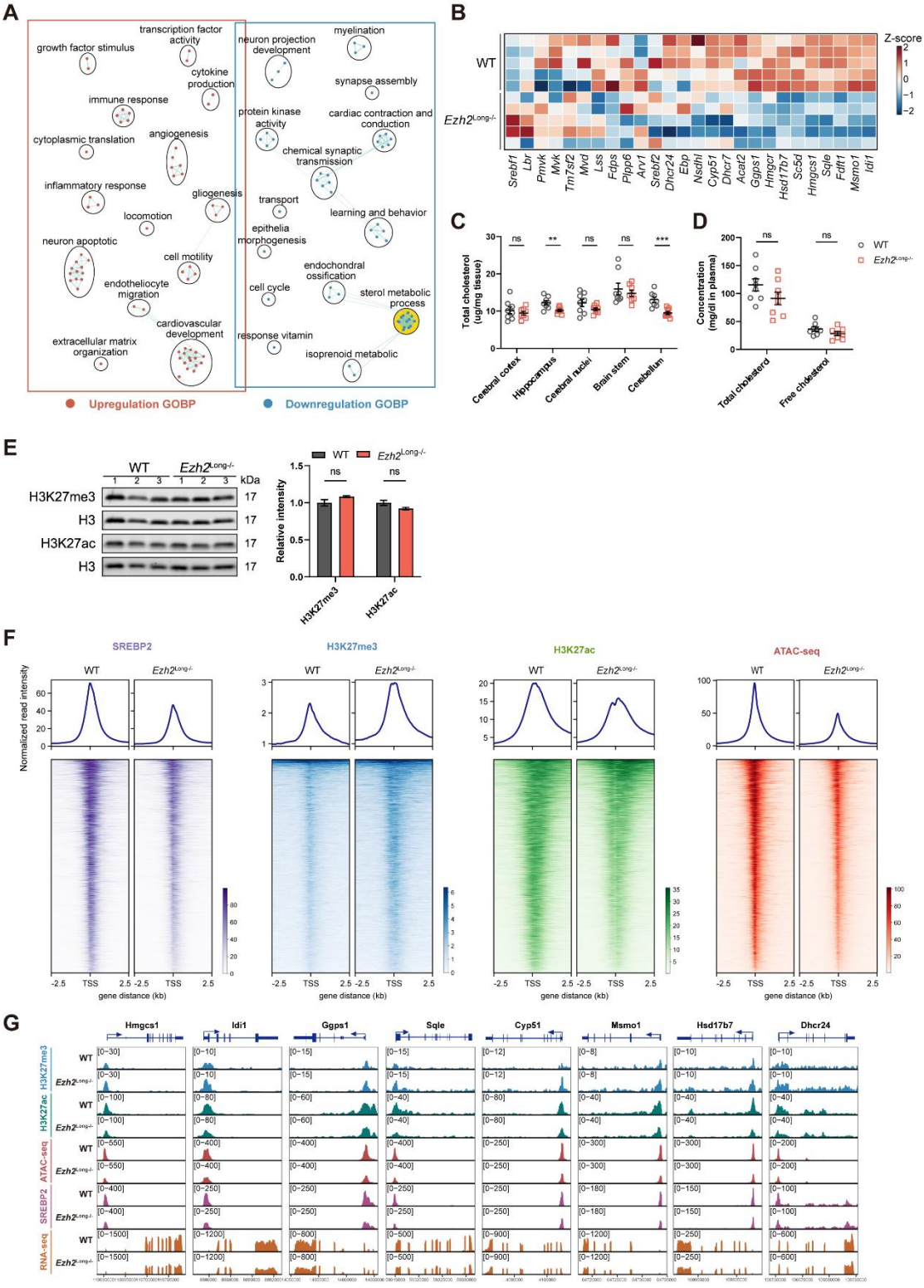

Figure S2. Loss of *Ezh2*^{Long} impairs cholesterol biosynthesis.

(A) Enrichment map showing significantly enriched GO terms for genes with significantly upregulation or downregulation in *Ezh2*$^{Long-/-}$ mice. The size of the nodes represents the number of genes in a particular GO term. Highly related terms are grouped into a theme (black circle) and annotated manually. The number of genes shared between each GO term is indicated by green lines. **(B)** Heatmap showing the relative expression value (Z-score) of genes involved in cholesterol biosynthesis in WT (n = 5) and *Ezh2*$^{Long-/-}$ (n = 5) cerebellum according to RNA-seq data. **(C)** Quantification of total cholesterol levels in multiple brain regions from the WT (n = 8) and *Ezh2*$^{Long-/-}$ (n = 8) mice. Unpaired t test; ns, not significant; $^{**}p < 0.01$; $^{***}p < 0.001$. (**D**) Quantification of total cholesterol and free cholesterol levels in plasma from the WT (n = 8) and *Ezh2*$^{Long-/-}$ (n = 8) mice. Unpaired t test; ns, not significant. **(E)** Western blot analysis and quantification of H3K27me3 and H3K27ac in isolated WT (n = 3) and *Ezh2*$^{Long-/-}$ (n = 3) cerebellums. H3 was used as loading control. Unpaired t test; ns, not significant. **(F)** Heatmaps and metagene plots showing CUT&Tag-seq (SREBP2, H3K27me3 and H3K27ac) and ATAC-seq signal within ± 2.5 kb of the TSS at SREBP2 targeted genes in WT and *Ezh2*$^{Long-/-}$ mice. Genes within each heatmap are rank ordered from high to low SREBP2 occupancy in the WT mice. **(G)** Genome tracks showing CUT&Tag-seq (H3K27me3, H3K27ac and SREBP2), ATAC-seq and RNA-seq normalized coverage over representative cholesterol synthesis-related genes locus in WT and *Ezh2*$^{Long-/-}$ mice.

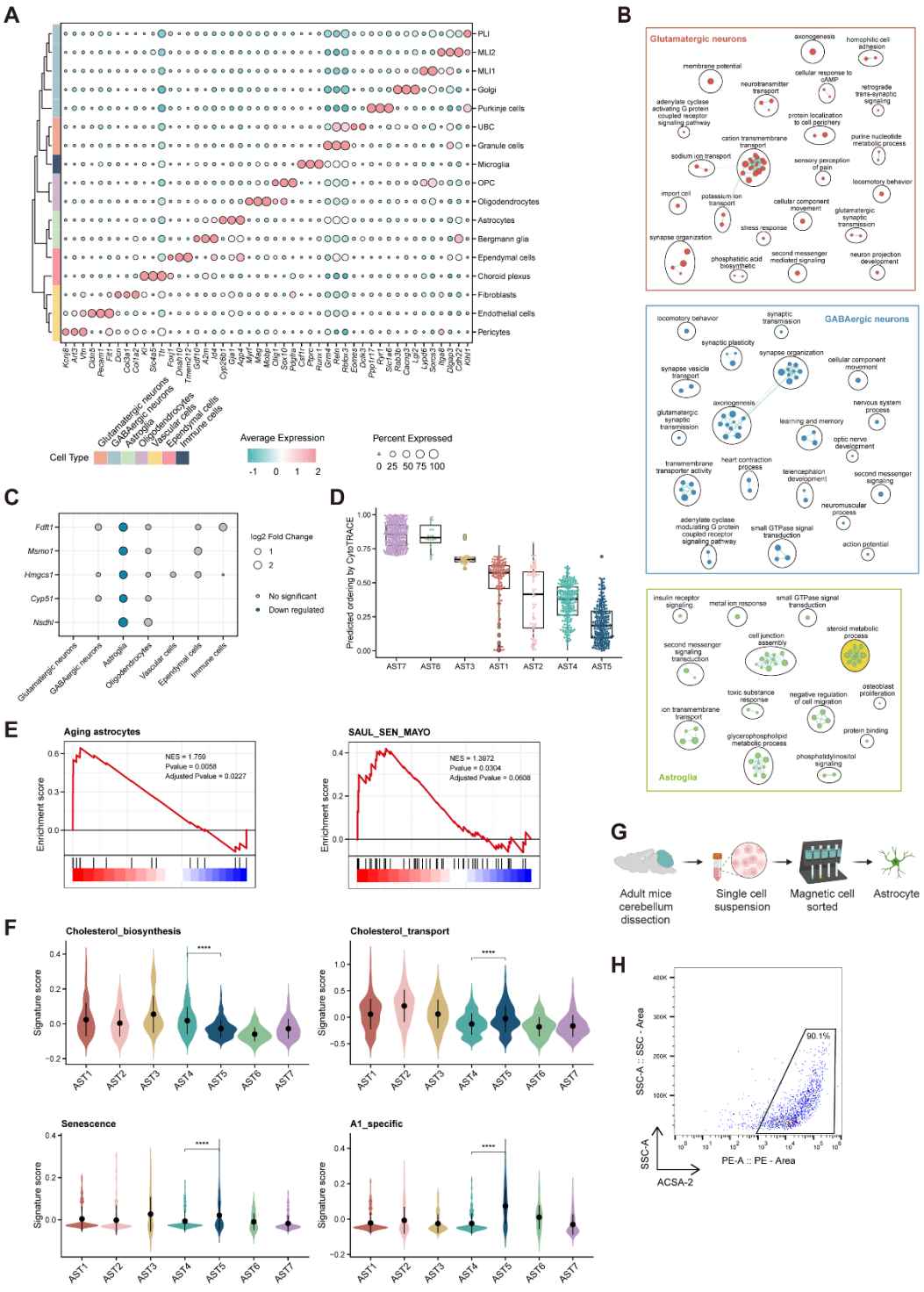

Figure S3. *Ezh2*$^{\text{Long-/-}}$ mice exhibit impaired astroglial cholesterol synthesis.

(A) Dendrogram showing hierarchical relationships between cell subtypes (left) with a paired dotplot (right) of average gene expression of selected marker genes for cell type identity. **(B)** Enrichment map showing significantly enriched GO terms for DEGs in broad cell types. The size of the nodes represents the number of genes in a particular GO term. Highly related terms are grouped into a theme (black circle) and annotated manually. The number of genes shared between each GO term is indicated by green lines. **(C)** Dotplots showing the relative expression change of specific genes involved in cholesterol synthesis across different cell types. The size indicates the

391 log_2 fold changes values (*Ezh2*$^{Long-/-}$ versus WT). **(D)** Boxplots showing differentiation potential for
392 astroglia subclusters predicted by CytoTRACE. **(E)** GSEA analysis of *Ezh2*$^{Long-/-}$ versus WT by
393 using two public signatures. Genes were ranked by expression fold change, with the most
394 upregulated genes on the left side of the plot and downregulated genes on the right. **(F)** Violin plots
395 displaying the gene scoring analysis of astroglia subclusters using the molecular signatures of gene
396 sets for cholesterol biosynthesis, cholesterol transport, senescence and A1-specific. Wilcoxon rank-
397 sum test; ****$p < 0.0001$. **(G)** Experimental flowchart for astrocytes isolation of murine cerebellum.
398 **(H)** Flow cytometric analysis of ACSA-2$^+$ astrocytes (gated in black polygon) collected after
399 microbeads kit separation.

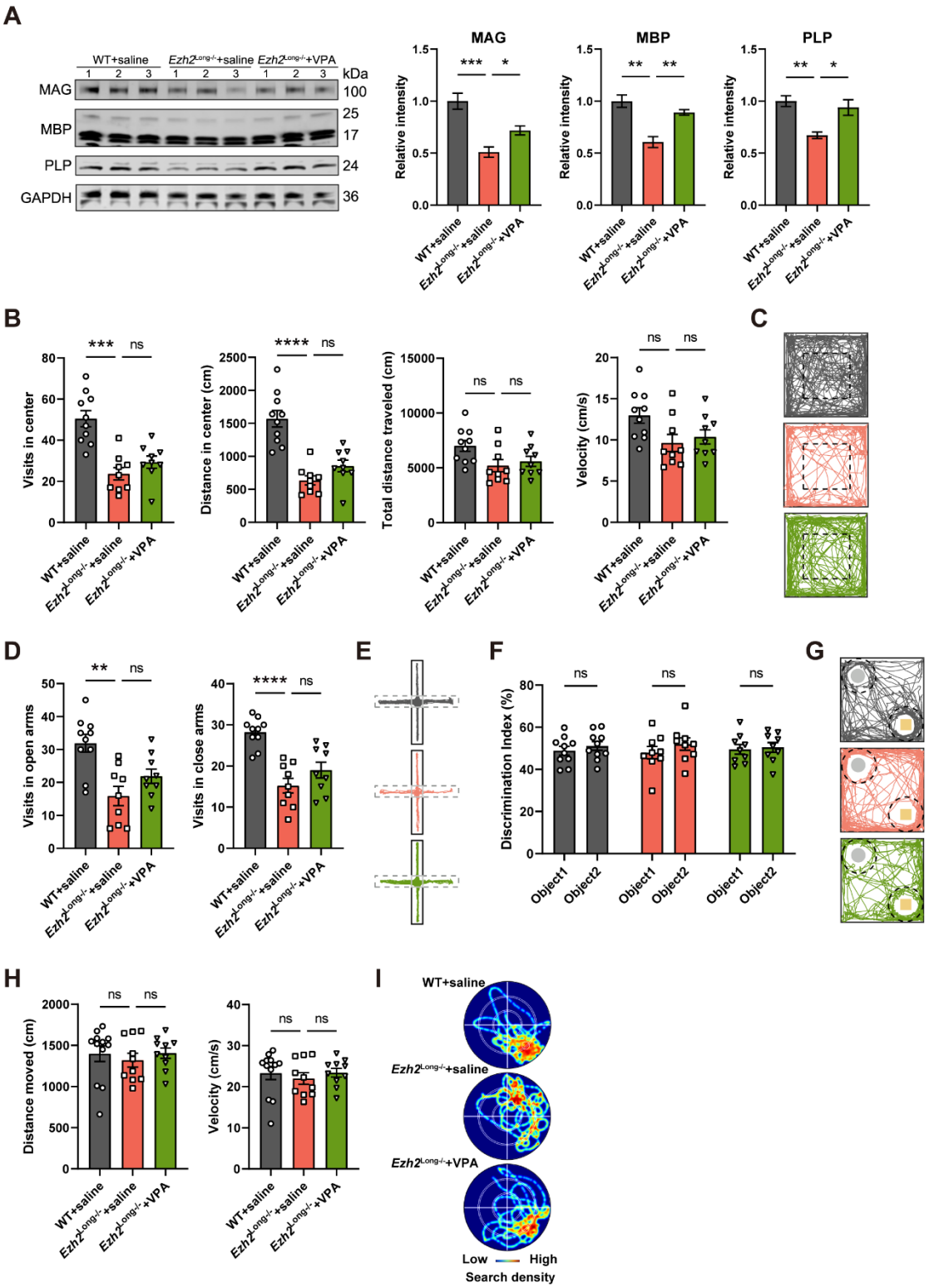

Figure S4. Valproic acid alleviates neurological impairments in *Ezh2*$^{Long-/-}$ mice.

(A) Western blot analysis and quantification of MAG, MBP and PLP in isolated murine cerebellums (WT + saline, n = 6; *Ezh2*$^{Long-/-}$ + saline, n = 6; *Ezh2*$^{Long-/-}$ + VPA, n = 6). GAPDH was used as loading control. Unpaired t test; *$p < 0.05$; **$p < 0.01$; ***$p < 0.001$. **(B)** Open field test showing comparable exploratory locomotor activity among saline-treated WT, saline-treated *Ezh2*$^{Long-/-}$ and VPA-treated *Ezh2*$^{Long-/-}$ mice. (WT + saline, n = 10; *Ezh2*$^{Long-/-}$ + saline, n = 9; *Ezh2*$^{Long-/-}$ + VPA, n

= 9). One-way ANOVA; ns, not significant; ***$p < 0.001$; ****$p < 0.0001$. **(C)** Representative movement trajectories of saline-treated WT, saline-treated *Ezh2*$^{Long-/-}$ and VPA-treated *Ezh2*$^{Long-/-}$ mice in the open field test. **(D)** Elevated plus maze test showing the numbers of entries into the open and closed arms in saline-treated WT, saline-treated *Ezh2*$^{Long-/-}$ and VPA-treated *Ezh2*$^{Long-/-}$ mice. (WT + saline, n = 10; *Ezh2*$^{Long-/-}$ + saline, n = 9; *Ezh2*$^{Long-/-}$ + VPA, n = 9). One-way ANOVA; ns, not significant; **$p < 0.01$; ****$p < 0.0001$. **(E)** Representative movement trajectories of saline-treated WT, saline-treated *Ezh2*$^{Long-/-}$ and VPA-treated *Ezh2*$^{Long-/-}$ mice in the elevated plus maze test. **(F)** Groups of mice have no preference for the same objects in the experimental box during the training period of NORT (WT + saline, n = 10; *Ezh2*$^{Long-/-}$ + saline, n = 9; *Ezh2*$^{Long-/-}$ + VPA, n = 9). Two-way ANOVA; ns, not significant. **(G)** Representative movement trajectories of saline-treated WT, saline-treated *Ezh2*$^{Long-/-}$ and VPA-treated *Ezh2*$^{Long-/-}$ mice during the test period of NORT. **(H)** Comparable locomotor ability among saline-treated WT, saline-treated *Ezh2*$^{Long-/-}$ and VPA-treated *Ezh2*$^{Long-/-}$ mice during the probe trial of MWMT (WT + saline, n = 12; *Ezh2*$^{Long-/-}$ + saline, n = 10; *Ezh2*$^{Long-/-}$ + VPA, n = 10). One-way ANOVA; ns, not significant. **(I)** Representative density plot of probe trial in saline-treated WT, saline-treated *Ezh2*$^{Long-/-}$ and VPA-treated *Ezh2*$^{Long-/-}$ mice. Red zones display the areas mostly explored by the mice.

Table S1. Primer sequences for genotyping and quantitative real-time PCR.

Target	Primer name	Application	Sequences (5'-3')
Ezh2$^{Long-/-}$	*Ezh2*$^{Long-/-}$ F1	genotyping	5'-GAGTGTGGAGAATTGTAGTATCTTGTGTGAATCTGT-3'
	Ezh2$^{Long-/-}$ R1		5'-GAGAGACATCCTGAAGTCTGTGAATTCTTC-3'
Ezh2$^{Long-/-}$	*Ezh2*$^{Long-/-}$ F2	genotyping	5'-TTGAGAATTGTTGCAACACTGTGTTAACCAAC-3'
	Ezh2$^{Long-/-}$ R2		5'-ATTGCGCGGGACTAGGGAGC-3'
Gapdh	*Gapdh* F	real-time PCR	5'-GGTGAAGGTCGGTGTGAACG-3'
	Gapdh R		5'-CTCGCTCCTGGAAGATGGTG-3'
Ezh2	*Ezh2* F	real-time PCR	5'-GAGTGGAAGCAGCGGAGGAT-3'
	Ezh2 R		5'-TGTAAGGGCGACCAAGAGTA-3'
Ezh2^{Long}	*Ezh2*^{Long} F	real-time PCR	5'-CGGGACTAGGGAGTGTTCAG-3'
	Ezh2^{Long} R		5'-ACATTATAGGCACCGAGGCG-3'
Ezh2^{Short}	*Ezh2*^{Short} F	real-time PCR	5'-CATGACTTCTTGTTCAGTCACCAG-3'
	Ezh2^{Short} R		5'-AATTCTGTTGTAAGGGCGACCA-3'
Cyp51	*Cyp51* F	real-time PCR	5'-CAACTCAACGAGAAGGTGGCT-3'
	Cyp51 R		5'-CTATCCCTGCGCCTGAAAC-3'

Fdft1	*Fdft1* F *Fdft1* R	real-time PCR	5’-GGGAATTGGCCTTTCTCGTC-3’ 5’-TAATGTATCTGCCCCACACCTCC-3’
Msmo1	*Msmo1* F *Msmo1* R	real-time PCR	5’-TCACGAGTTTCAGGCTCCA-3’ 5’-CATGCCCACAGGAGAATTACG-3’
Hmgcs1	*Hmgcs1* F *Hmgcs1* R	real-time PCR	5’-TATGATTGCATTGGGCGGCTA-3’ 5’-CTACCAGAGCATATCGTCCATCC-3’
Nsdhl	*Nsdhl* F *Nsdhl* R	real-time PCR	5’-AGTGTCTAAACCGGGAAGAAG-3’ 5’-CAAATGTGTTCCTGTGACCTGG-3’
Ggps1	*Ggps1* F *Ggps1* R	real-time PCR	5’-GACAACACTAACCATCACAGAGTG-3’ 5’-ACTATGACACCTCTGGCAAGC-3’
Hsd17b7	*Hsd17b7* F *Hsd17b7* R	real-time PCR	5’-GGCCACTTTATTCTGATTCGGG-3’ 5’-AAGCCACATTCAGGAGGTCG-3’
Sqle	*Sqle* F *Sqle* R	real-time PCR	5’-TTGCGGATGGACTCTTCTCC-3’ 5’-AACTGTGGTGCATCCTTCAT-3’
Hmgcr	*Hmgcr* F *Hmgcr* R	real-time PCR	5’-CCCTCAGTTCAAATTCACAGGATG-3’ 5’-CAAGGCATTCCACAAGAGCG-3’
Sc5d	*Sc5d* F *Sc5d* R	real-time PCR	5’-GGAGACTTTCCAAATGGCTGGA-3’ 5’-GGTGCAGGCCCCTATGAATC-3’
Dhcr7	*Dhcr7* F *Dhcr7* R	real-time PCR	5’-TTAACCTGTCCTTCGCTGCC-3’ 5’-CTAACACGTAGATGGCCTGCAA-3’
Trp53	*Trp53* F *Trp53* R	real-time PCR	5’-TCCGAAGACTGGATGACTGC-3’ 5’-CCTGAAAATGTCTCCTGGCTCA-3’
Cdkn1a	*Cdkn1a* F *Cdkn1a* R	real-time PCR	5’-CAGACCAGCCTGACAGATTTCTA-3’ 5’-GAGGGCTAAGGCCGAAGATG-3’
Lcn2	*Lcn2* F *Lcn2* R	real-time PCR	5’-CCACCACGGACTACAACCA-3’ 5’-ACAGCTCCTTGGTTCTTCCATAC-3’

425